Supporting Information

McConnell et al. 10.1073/pnas.0902018106

SI Methods

ISH. ISH studies were performed using the *H2-K*^{b} probe 3′-TGTAGGCTATGTGG ACGACACGGAGTTCGTGCGCT-TCGACAGCGACGCGGAGAATCCGAGATATGAGCC-GCGGGCGCGGTGGATGGAGCAGGAGGGGCCCGA-GTATTGGGAGCGGGAGACACAGAAAGCCAAGGGC-AATGAGCAGAGTTTCCGAGTGGACCTGAGGACCC-TGCTCGGCTACTACAACCAGAGCAAGGGCGGCTC-TCACACTATTCAGGTGATCTCTGGCTGTGAAGTG-GGGTCCGACGGGCGACTCCTCCGCGGGTACCAGC-AGTACGCCTACGACGGCTGCGATTACATCGCCCT-GAACGAGGACCCAC-5′ and the *H2-D*^{b} probe 3′-AGGTG-GGCTACGTGGACGACGAGGAGTT CGTGCGCTTCGA-CAGCGACGCGGAGAATCCGAGATATGAGCCGCGG-GCGCCGTGGATGGAGCAGGAGGGGCCGGAGTAT-TGGGAGCGGGAAACACAGAAAGCCAAGGGCCAA-GAGCAGTGGTTCCGAGTGAGCCTGAGGAACCTG-CTCGGCTACTACAACCAGAGCGCGGGCGGCTCTC-ACACACTCCAGCAGATGTCTGGCTGTGACTTGGG-GTCGGACTGGCGCCTCCTCCGCGGGTACCTGCAG-TTCGCCTATGAAGGCCGCGATTACATCGCCCTGA-ACGAGAACCCAC-5′. For FISH, sections were prepared and processed as described for isotopic ISH (1) without ethanol dehydration. After hybridization, sections were washed for 10 min in 5× saline sodium citrate solution (SSC) at 62 °C, 3 times for 30 min in 0.2× SSC at 62 °C, and for 5 min in 0.2× SSC at room temperature. Sections were then transferred to 0.1 M Tris-buffered saline solution, pH 7.5 (TBS) for 5 min, followed by blocking with 10% sheep serum in TBS with 0.05% Tween-20 (TBS-T) for 60 min. H2-K^b probe was detected first by overnight incubation at 4 °C with HRP-conjugated anti-fluorescein antibody (1 426 346; Roche Diagnostics; 1:1,000). The next day, sections were rinsed 3 times for 10 min in 0.1 M TBS-T followed by tyramide signal amplification using fluorescein-tyramide substrate diluted 1:100 in amplification buffer for 3 to 10 min in dark (NEL701; Perkin-Elmer). Next, sections were rinsed in TBS-T and residual peroxidase was quenched using 0.3% H_2O_2 for 1 to 3 min. H2-D^b probe was detected similarly using HRP-conjugated anti-digoxigenin (1 207 733; Roche Diagnostics; 1:1,000) and Cy3-tyramide (NEL704A; Perkin-Elmer). Slides were mounted using Prolong Gold (P36930; Molecular Probes).

CF Synapse Distribution Analysis. Analysis of CF synaptic puncta was performed on 50-μm sections of the cerebellar vermis, in the bank regions of lobules VI and VII, of postnatal d 21 to 23 male mice perfused and sliced as described (see *Materials and Methods* in the main text). Blocking with was performed in 10% horse serum (HS) in PBS-T for 1 h; then sections were incubated at 4 °C overnight with 1° antibody. Primary antibodies were mouse anti-mouse calbindin (C9848; Sigma-Aldrich; 1:500) and guinea pig anti-mouse vGluT2 (AB2251; Chemicon, 1:2,500) in 10% HS in PBS-T. Following three 30-min washes in PBS-T, bound 1° antibodies were detected using Texas Red-conjugated anti-mouse IgG (715–075-150; Jackson ImmunoResearch) and Cy2-conjugated anti-guinea pig IgG (706–225-140; Jackson ImmunoResearch), each diluted 1:500 in 10% HS, washed again, and mounted using Prolong Gold. Unless indicated otherwise, reagents were obtained from Sigma-Aldrich. Fluorescent micrographs were obtained from projected confocal image stacks (LSM510 META; Carl Zeiss) and filtered to maximize the dynamic range and sharpness using LSM image manager (Carl Zeiss).

The number and distribution of vGluT2 puncta were counted using a homemade MatLab script (MathWorks). Images from 3 to 4 WT and 3 to 4 KO animals were pooled and blinded, and an analysis threshold was chosen manually by visual comparison with 3 to 4 images before all images from a given pool were analyzed at that threshold. For each image, the basal and pial border of the molecular layer (ML) were identified in a graphical user interface. The basal, middle, and pial thirds of the ML were determined by extrapolating 10 orthogonal points [supporting information (SI) Fig. S2*D*, pink and blue circles] in the center 40% of each border; these points are 33% of the distance from one border to the opposite border. Regions were subdivided based on best-fit lines from the image edges through the 10 extrapolated points. Puncta within each region were counted and normalized to the thickness and area of each region.

PC Dendrite Analysis. In 250-μm slices prepared for physiological experiments (see *Materials and Methods* in the main text), 1 to 4 PCs were filled with 2% Lucifer yellow (L0259; Sigma-Aldrich) diluted in potassium-based internal solution. Sections were immersion fixed in 4% paraformaldehyde at 4 °C overnight. Immunostaining for Lucifer yellow was performed as described for vGluT2 earlier by using an anti-Lucifer yellow primary antibody (L9163; Sigma-Aldrich; 1:1,000) and Cy2-conjugated donkey anti-rabbit secondary antibody (711–225-152; Jackson ImmunoResearch; 1:500). Confocal image stacks were obtained as described for vGluT2 immunostained sections, and PC dendritic arbors were traced using Neurolucida (MBF Bioscience). Sholl and segment length analysis were performed in Excel on data generated in Neurolucida. Kolmogorov-Smirnov tests were performed in MatLab.

Flow Cytometry. Red blood cells were lysed from crushed spleens according to manufacturer's instructions (red blood cell lysing buffer, R7757; Sigma-Aldrich). Residual cells, splenocytes, were kept on ice. One million cells were used per experimental condition. Incubations were performed at 4 °C and washes were performed at room temperature. Cells were incubated in FACS buffer (PBS solution plus 10% goat serum, 5% FBS, 5% horse serum, 2 mM EDTA) with Fc Block (553141; PharMingen; 1:100) for 30 min, then 2 μg/mL ErHr52 (BMA Biochemicals) or rat IgG2 (AbD Serotec) diluted in FACS buffer for 30 min. Three 5-min washes were performed; then cells were incubated with secondary antibody, FITC-conjugated goat F(ab′)2 anti-rat (STAR69; 1:300; AbD Serotec), for 30 min. Three final 5-min washes were performed before analysis. Cellular debris and dead cells were excluded from analysis by gating, and 10,000 cells were analyzed per condition on a FACS (Becton-Dickinson).

Additional Animals. An in-house C57BL/6 WT line is denoted $\beta2m^{+/+}TAP1^{+/+}CD3\zeta^{+/+}$; these mice are controls for $\beta2m^{-/-}TAP1^{-/-}$ and $CD3\zeta^{-/-}$ lines as described previously (2). To avoid genetic drift and provide ideal congenic control, $\beta2m^{-/-}$, $TAP1^{-/-}$, $\beta2m^{-/-}TAP1^{-/-}$, and the in-house C57 WT line are maintained as a mixed heterozygote colony. $PirB^{+/+}$ and $PirB^{\Delta/\Delta}$ lines are maintained by heterozygote breeding and are a C57 × 129 background (3). All protocols were approved by the Harvard Medical School and Stanford University Animal Care and Use Committees.

Open-Field and Elevated Plus Maze. Open-field and elevated plus maze studies were performed exactly as described previously (4, 5). Naive 8- to 10-week-old mice were tested first in the open-field maze; 24 h later they were tested in the elevated plus maze. A TSE Mot video tracking system (TSE Systems) was used to monitor animal movement for 5 min in a 50 × 35 cm^2 open-field maze or a H-10^{-35} elevated plus maze (Coulbourn Instruments).

1. Syken J, Shatz CJ (2003) Expression of T cell receptor beta locus in central nervous system neurons. *Proc Natl Acad Sci USA* 100:13048–13053.
2. Huh GS, et al. (2000) Functional requirement for class I MHC in CNS development and plasticity. *Science* 290:2155–2159.
3. Syken J, Grandpre T, Kanold PO, Shatz CJ (2006) PirB restricts ocular-dominance plasticity in visual cortex. *Science* 313:1795–1800.
4. Park SK, et al. (2005) Par-4 links dopamine signaling and depression. *Cell* 122:275–287.
5. Fischer A, Sananbenesi F, Pang PT, Lu B, Tsai LH (2005) Opposing roles of transient and prolonged expression of p25 in synaptic plasticity and hippocampus-dependent memory. *Neuron* 48:825–838.

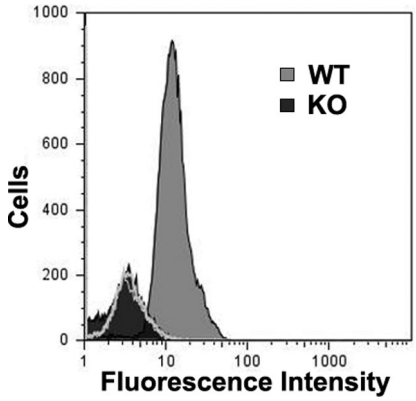

Fig. S1. Specific binding of ErHr52 antibody. Flow cytometric analysis of splenocytes from WT and $K^bD^{b-/-}$ (KO) mice. Fluorescence intensity is plotted across the *x* axis, the number of cells is plotted on the *y* axis. WT cells (gray region) show strong binding by ErHr52 (i.e., high fluorescence intensity). However, ErHr52 binding to $K^bD^{b-/-}$ cells (black region) is comparable to that observed with isotype control antibodies on WT (thin gray line) or $K^bD^{b-/-}$ (thick gray line) cells.

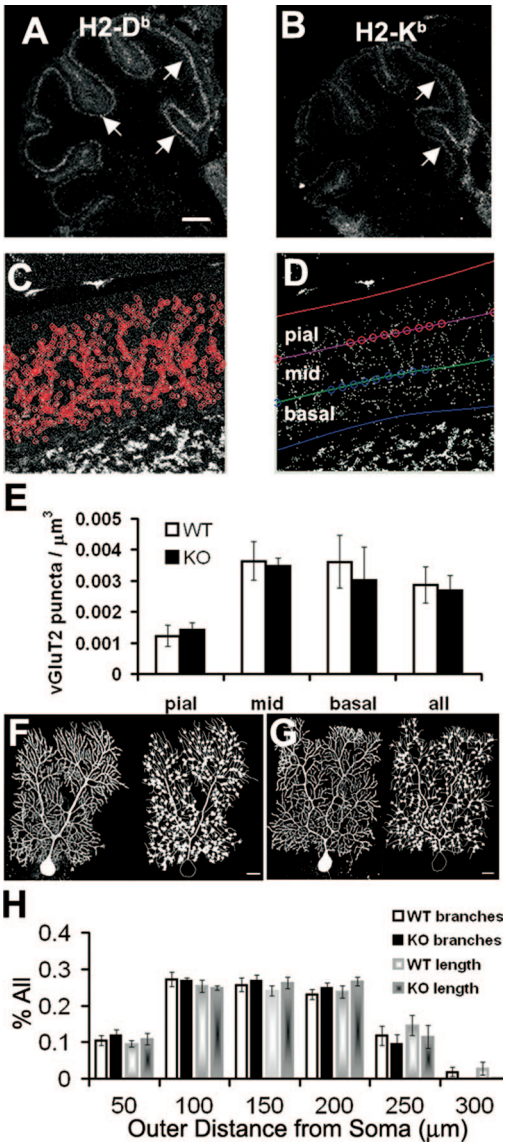

Fig. S2. $K^bD^{b-/-}$ CF synapses and PC dendritic arbors are similar to WT. (*A* and *B*) Dark-field micrographs of P7 WT sagittal cerebellar sections show MHCI expression during development. (*A*) Hybridization of pattern obtained with H2-D^b riboprobe indicates expression in PC layer (white arrows). (*B*) Hybridization of pattern obtained with H2-K^b riboprobe indicates expression in PC layer (white arrows). (Scale bar, 400 μm.) (*C–E*) Thresholded green channel images were used to count vGluT2 immunoreactive puncta (*C*, red circles) in the pial, middle, and basal thirds of the ML (*D*). (*E*) Bar graphs present the average density of puncta, from the depth of image stacks, present in each third or in the entire (*all*) ML. Average density is plotted on the *y* axis for each group as labeled. (*F–H*) A representative WT PC dendritic arbor (*F*, *Left*), traced (*F*, *Right*) to analyze branching. (Scale bar, 20 μm.) (*G*) A representative $K^bD^{-/-}$ PC dendritic arbor (*Left*), traced (*Right*) to analyze branching. (*F* and *G*) White dots indicate branch points. (Scale bar, 20 μm.) (*H*) Bar graphs present Sholl analysis of 7 WT and 7 $K^bD^{b-/-}$ PC arbors for the average number of branch points [white (WT) and black ($K^bD^{b-/-}$) bars] and the total dendritic length [shaded white (WT) and shaded black ($K^bD^{b-/-}$) bars] counted in 50-μm bins from the soma. The *y* axis indicates the average ± SEM, and the *x* axis indicates the distance from the soma.

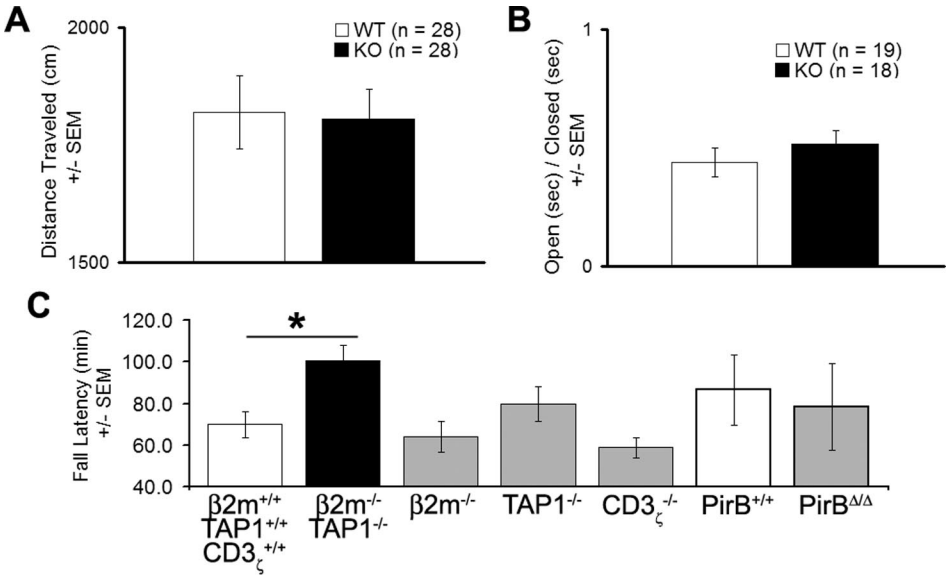

Fig. S3. Additional behavioral analyses in mice with abrogated MHCI function. (*A*) Open-field activity in WT (white bar) and $K^bD^{b-/-}$ (KO, black bar) mice is indistinguishable ($P = 0.871$) during 5 min in an open field. The average distance traveled by each strain is indicated on the *y* axis. (*B*) Elevated plus maze behavior is indistinguishable ($P = 0.378$) between WT (white bar) and $K^bD^{b-/-}$ (black bar) mice. A bar graph indicates the ratio (*y* axis) of time spent in the open versus closed arms of the maze. (*C*) Day 3 Rotarod performance (*y* axis) is significantly improved in $\beta2m^{-/-}Tap1^{-/-}$ (black bar; $n = 33$; *, $P < 0.003$ vs. $\beta2m^{+/+}TAP1^{+/+}CD3_\zeta^{+/+}$), but not related immunocompromised mouse strains (gray bars; $n = 17$ $\beta2m^{-/-}$, $P = 0.558$; $n = 25$ $TAP1^{-/-}$, $P = 0.331$) relative to WT cohorts (white bars; $n = 30$ $\beta2m^{+/+}TAP1^{+/+}CD3_\zeta^{+/+}$). Normal Rotarod performance is also observed in other mice with altered MHCI-related immunity (gray bars; $n = 10$ $CD3_\zeta^{-/-}$, $P = 0.332$; $n = 6$ $PirB^{\Delta/\Delta}$, $P = 0.768$ vs. $n = 7$ $PirB^{+/+}$). $CD3_\zeta^{-/-}$ mice are null for an integral component of T cell receptor signaling and $PirB^{\Delta/\Delta}$ mice lack functional alleles for another MHCI receptor (see main text for additional description and references).

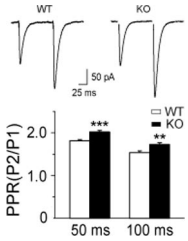

Fig. S4. Altered basal transmission at PF synapses in $K^bD^{b-/-}$ mice. PF EPSCs exhibit enhanced paired-pulse facilitation in $K^bD^{b-/-}$ mice. Example traces of paired PF EPSCs (*Upper*) and grouped data (*Lower*) show the mean PPR at 50 ms ISI (WT, 1.81 ± 0.03, $n = 22$ cells; $K^bD^{b-/-}$, 2.02 ± 0.03, $n = 24$) and 100 ms inter-stimulus intervals in the 2 genotypes (WT, 1.54 ± 0.04, $n = 12$; $K^bD^{b-/-}$, 1.72 ± 0.05, $n = 7$), recorded at room temperature. Holding potential was −65 mV. (**, $P < 0.01$; ***, $P < 0.001$).

Table S1. CF EPSC analysis

	WT ($n = 11$)	KO ($n = 16$)	P value
Peak amplitude (at −10 mV), pA	−903 ± 71	−1,011 ± 63	0.271
Rise time (10–90%), ms	1.00 ± 0.04	0.86 ± 0.08	0.136
Decay time (100–50%), ms	10.3 ± 0.6	10.8 ± 0.3	0.457

Results are presented as mean ± SEM.

Table S2. CF complex spike analysis

	WT (n = 13)	KO (n = 15)	P value
Baseline (50 ms before stimulation), mV	−65.8 ± 0.6	−65.6 ± 0.8	0.808
No. of spikelets	3.6 ± 0.2	3.6 ± 0.2	0.950
Peak amplitude of spikelets, mV			
1	75.1 ± 2.7	76.7 ± 2.7	0.682
2	48.8 ± 3.0	46.2 ± 2.6	0.582
3	51.4 ± 3.1	45.7 ± 2.4	0.156
4	32.1 ± 7.2	32.5 ± 5.7	0.965
5	52.1 (n = 1/13)	45.9 (n = 1/15)	
Afterhyperpolariztion, mV	−1.8 ± 0.2	−2.0 ± 0.2	0.505

Results are presented as mean ± SEM.